Propagation characteristics of hybrid modes supported by metal-low-high index waveguides and bends

M. Z. Alam*, J. Meier, J. S. Aitchison, and M. Mojahedi

Department of electrical and computer engineering, University of Toronto, Toronto, Ontario, M5S 3G4, Canada
**malam@waves.utoronto.ca*

Abstract: Hybrid-mode waveguides consisting of a metal surface separated from a high index medium by a low index spacer have attracted much interest recently. Power is concentrated in the low index spacer region for this waveguide. Here we investigate the properties of the hybrid mode in detail and numerically demonstrate the possibility of realizing compact waveguide bends using this wave guiding scheme.

OCIS codes: (130.3120) Integrated optics devices; (130.2790) Guided waves; (240.6680) Surface plasmons.

References and links

1. W. L. Barnes, A. Dereux, and T. W. Ebbesen, "Surface plasmon subwavelength optics," Nature **424**(6950), 824–830 (2003).
2. J. Homola, "Present and future of surface plasmon resonance biosensors," Anal. Bioanal. Chem. **377**(3), 528–539 (2003).
3. J. Takahara, S. Yamagishi, H. Taki, A. Morimoto, and T. Kobayashi, "Guiding of a one-dimensional optical beam with nanometer diameter," Opt. Lett. **22**(7), 475–477 (1997).
4. E. Ozbay, "Plasmonics: merging photonics and electronics at nanoscale dimensions," Science **311**(5758), 189–193 (2006).
5. J. A. Dionne, L. A. Sweatlock, H. A. Atwater, and A. Polman, "Plasmon slot waveguides: Towards chip-scale propagation with subwavelength-scale localization," Phys. Rev. B **73**(3), 035407 (2006).
6. G. Veronis, and S. Fan, "Guided subwavelength plasmonic mode supported by a slot in a thin metal film," Opt. Lett. **30**(24), 3359–3361 (2005).
7. A. Boltasseva, T. Nikolajsen, K. Leosson, K. Kjaer, M. S. Larsen, and S. I. Bozhevolnyi, "Integrated optical components utilizing long-range surface plasmon polaritons," J. Lightwave Technol. **23**(1), 413–422 (2005).
8. S. I. Bozhevolnyi, V. S. Volkov, E. Devaux, J.-Y. Laluet, and T. W. Ebbesen, "Channel plasmon subwavelength waveguide components including interferometers and ring resonators," Nature **440**(7083), 508–511 (2006).
9. B. Steinberger, A. Hohenau, H. Ditlbacher, A. L. Stepanov, A. Drezet, F. R. Aussenegg, A. Leitner, and J. R. Krenn, "Dielectric stripe on gold as surface plasmon waveguides," Appl. Phys. Lett. **88**(9), 094104 (2006).
10. M. Yan, M. Qiu, "Compact optical waveguides based on hybrid index and surface-plasmon-polariton guidance mechanisms," Act. Passive Electron. Compon. 52461, (2007).
11. M. Z. Alam, J. Meier, J. S. Aitchison, and M. Mojahedi, "Super mode propagation in low index medium," CLEO/QELS 2007, *http://www.opticsinfobase.org/abstract.cfm?uri=CLEO-2007-JThD112*.
12. R. F. Oulton, V. J. Sorger, D. A. Genov, D. F. P. Pile, and X. Zhang, "A hybrid plasmonic waveguide for subwavelength confinement and long range propagation," Nat. Photonics **2**(8), 496–500 (2008).
13. M. Fujii, J. Leuthold, and W. Freude, "Dispersion relation and loss of sub-wavelength confined mode of metal-dielectric-gap optical waveguides," IEEE Photon. Technol. Lett. **21**(6), 362–364 (2009).
14. D. Dai, and S. He, "A silicon-based hybrid plasmonic waveguide with a metal cap for a nano-scale light confinement," Opt. Express **17**(19), 16646–16653 (2009).
15. R. F. Oulton, G. Bartal, D. F. Pile, and X. Zhang, "Confinement and propagation characteristics of subwavelength plasmonic modes," N. J. Phys. **10**(10), 105018 (2008).
16. R. Buckley, and P. Berini, "Figures of merit for 2D surface plasmon waveguides and application to metal stripes," Opt. Express **15**(19), 12174–12182 (2007).
17. P. B. Johnson, and R. W. Christy, "Optical constants of noble metals," Phys. Rev. B **6**(12), 4370–4379 (1972).
18. J. A. Dionne, L. A. Sweatlock, H. A. Atwater, and A. Polman, "Planar metal plasmon waveguides: frequency-dependent dispersion, propagation, localization, and loss beyond the free electron model," Phys. Rev. B **72**(7), 075405 (2005).
19. *Electromagnetics Module User's Guide* (Comsol, 2007).
20. E. D. Palik, *Handbook of optical constants of solids*, (Academic Press, Inc. 1985).
21. H. Raether, Surface plasmons on smooth and rough surfaces and on gratings, (Springer, Berlin, 1988).
22. *FDTD Solutions Reference Guide*, (Lumerical Solutions, 2009).

#125806 - $15.00 USD Received 22 Mar 2010; revised 13 Apr 2010; accepted 13 Apr 2010; published 2 Jun 2010

1. Introduction

Surface plasmons (SP) offer some unique features which can be useful for many different applications [1]; for example SP based biosensing is already a well established and commercially successful technology [2]. Another motivation behind the growing interest in plasmonics is the potential for the realization of very compact photonic devices which is not possible using a conventional index guiding scheme [3]. Plasmonics is considered as a potential solution for the size mismatch problem of electronics and photonics [4].

One of the biggest challenges preventing wide spread use of plasmonic technology is the significant loss suffered by SP. At visible and near infrared wavelengths metals have a complex permittivity and as a result SP suffers very high attenuation. In an attempt to obtain a satisfactory compromise between loss and confinement, different plasmonic waveguide designs such as metal-insulator-metal [5], metal slot [6], insulator-metal-insulator [7] and channel waveguides [8] have been proposed. Moreover, in recent years, hybrid wave guiding schemes have received an increasing amount of attention [9–15]. For these structures the wave guiding mechanism consists of a combination of plasmon and index guiding. One particular structure that is the focus of much interest is the hybrid waveguide consisting of a high index medium separated from a metal surface by a low index spacer [11–14]. It has been shown that this waveguide can provide a good compromise between confinement and propagation distance [12].

Here we extend our earlier work on hybrid waveguides [11] and examine the properties of the hybrid mode and its potential application for realizing compact waveguide bends. To be able to properly design bends and other components, a clear understanding of the hybrid mode characteristics is necessary. Therefore, in section 2 we investigate the properties of such modes and examine the mode profile of a four layer structure of infinite width. For nano-photonic applications good two-dimensional confinement is necessary and a finite width structure will be more useful. Therefore, we also analyze the mode characteristics of the structure reported in [11] and [13] and identify a number of advantages of the hybrid wave guiding scheme. In section 3 we present the design of a compact waveguide bend. Section 4 contains our conclusion and final remarks.

2. Analysis of the modes supported by hybrid waveguide

The key performance criteria for a plasmonic waveguide are the propagation distance and confinement of the guided mode. While the propagation distance is a well defined quantity, the evaluation of confinement is more complicated. R. F. Oulton *et al.* [15] and R. Buckley *et al.* [16] have discussed in detail various ways of evaluating mode confinement. The choice of confinement measure is dependent on the specific application. Lateral field confinement is more important than vertical confinement for integrated optics while overall mode size may be more relevant for sensing applications. One objective of this paper is to examine the usefulness of the hybrid waveguide for integrated optics. We will use the *lateral distance* over which the transverse electric field drops to 1/e of its maximum magnitude as a measure of field confinement. Confinement in the lateral dimension has also been previously used by others as a measure of plasmonic guide performance [8, 9].

2.1 Analysis of the mode characteristics for an infinite width structure

The geometry of the 4-layer structure is shown in Fig. 1. The wave propagates along the z-direction and the structure is infinite in the x-direction. The bottom layer is silver and its properties are derived from Refs [17]. and [18]. The other three layers are lossless dielectrics with positive permittivity: ε_{spacer}, ε_{hi}, and ε_{cover}. We assume $\varepsilon_{spacer} < \varepsilon_{hi}$. The wavelength of operation is 0.8 μm. Carrying out the analysis at this wavelength lets us compare the performance of the hybrid guide to that of previously reported relevant work [9].

#125806 - $15.00 USD Received 22 Mar 2010; revised 13 Apr 2010; accepted 13 Apr 2010; published 2 Jun 2010

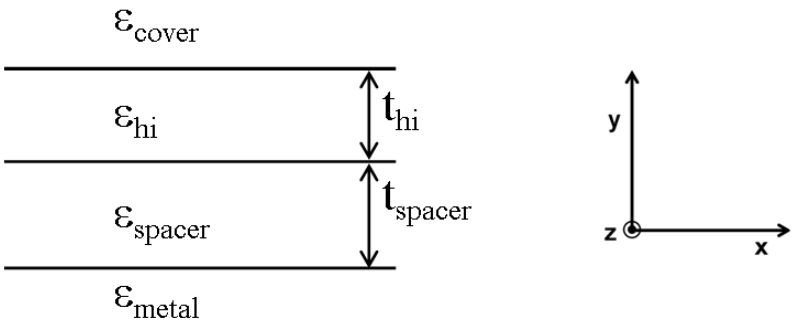

Fig. 1. Schematic of the infinite width hybrid waveguide and the coordinate system used.

To examine the field profile of the hybrid mode supported by the structure shown in Fig. 1 we have used Comsol Multiphysics - a commercially available finite element code. For the case under consideration, the code solves the following wave equation for the transverse magnetic field, $\vec{H}_t$ [19]:

$$\nabla_t \times (\varepsilon_{ri}^{-1} \nabla_t \times \vec{H}_t) - \nabla_t (\mu_{ri}^{-1} \nabla_t \vec{H}_t) - (k_0^2 \mu_{ri} - \beta^2) \vec{H}_t = 0 \qquad (1)$$

Here $\nabla_t = \hat{x}\frac{\partial}{\partial x} + \hat{y}\frac{\partial}{\partial x}$, β is the propagation constant and ε_{ri}, μ_{ri} are the relative permittivity and permeability of the medium *i* where *i* can be metal, spacer, high index, or cover region. Details of the solution process can be found in [19]. Figure 2 shows the magnitude of the normalized magnetic field intensity, electric field intensity, and guided power density of the hybrid mode for the dimensions and properties mentioned in figure caption. Since the hybrid mode is TM in nature, both transverse and longitudinal components of electric fields exists but the transverse field component E_y dominates. As shown in Fig. 2(a) and 2(b) the transverse component of electric field (E_y) and magnetic field (H_x) are highly concentrated in the low index spacer layer. Figure 2(c) shows the profile of the guided power of the hybrid mode. To compare the power confinement of the hybrid mode to that of single interface SP, power profile for the latter case is also shown in Fig. 2(c). In case of the single interface SP the metal is also silver and the permittivity of the dielectric medium adjacent to the metal is chosen to be 2.8 to make the propagation distance same as that of the hybrid mode. It can be seen that the hybrid mode provides a better confinement compared to the single interface SP mode for same propagation distance.

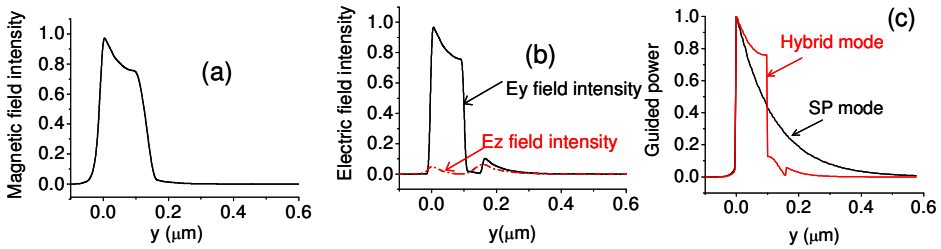

Fig. 2. Field intensity plots of hybrid mode for t_{spacer} = 100 nm and t_{hi} = 60 nm, ε_{spacer} = 2, ε_{hi} = 12, ε_{cover} = 1 (a) magnetic field, H_x (b) electric field E_y and E_z (c) guided power for hybrid mode and SP mode at silver dielectric interface. All quantities are normalized.

2.2 Analysis of the mode characteristics for a finite width structure

A finite width hybrid waveguide can be implemented in a number of ways [11–14]. Here we analyze the structure reported in [11] and [13] which is shown in Fig. 3. It consists of a high

#125806 - $15.00 USD Received 22 Mar 2010; revised 13 Apr 2010; accepted 13 Apr 2010; published 2 Jun 2010

index dielectric slab (permittivity ε_{hi}) of dimensions $w \times h$ separated from a metallic surface (permittivity ε_{metal}) via a spacer (permittivity ε_{spacer}) of dimensions $w \times d$. Permittivity of the cover layer around the guide is ε_{cover}. The spacer, high index and cover region are assumed to be silica, silicon and air, respectively and their material properties are taken from [20].

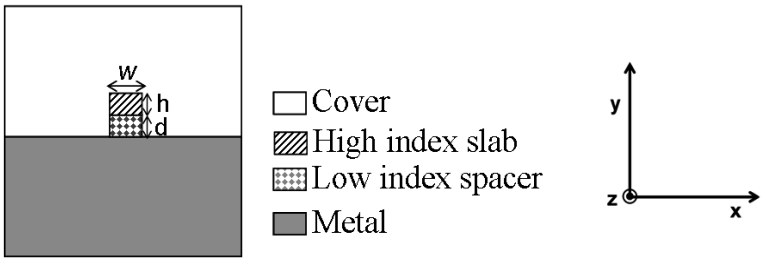

Fig. 3. Schematic of the two dimensional waveguide.

We have carried out a detailed study to investigate the effects of changing waveguide dimensions on the waveguide performance. Some of the results are shown in Fig. 4 and Fig. 5. The effective mode index n_{eff} is defined as $n_{eff} = k/k_0$ where k and k_0 are the propagation constant of the hybrid mode and free space wave number, respectively. The propagation distance is defined as the distance over which the guided power drops to 1/e of its initial magnitude. The mode size is defined as the distance over which the transverse electric field E_y along the metal-dielectric interface drops to 1/e of its maximum amplitude.

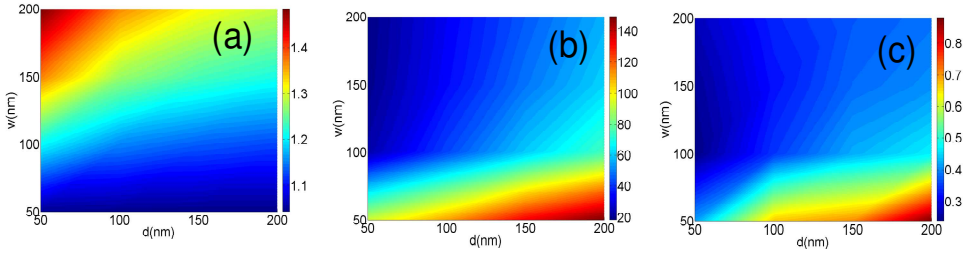

Fig. 4. Effects of varying waveguide width and spacer height for h = 60 nm, (a) real part of effective mode index (b) propagation distance (μm) (c) mode size (μm).

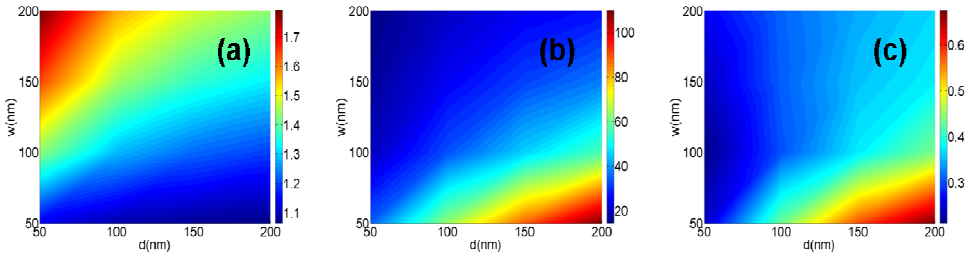

Fig. 5. Effects of varying waveguide width and spacer height for h = 100 nm, (a) real part of effective mode index (b) propagation distance (μm) (c) mode size (μm).

The trends shown in Fig. 4 and Fig. 5 were also observed for other choices of waveguide dimensions. Table 1 summarizes the effects of changing dimensions on waveguide performance.

#125806 - $15.00 USD Received 22 Mar 2010; revised 13 Apr 2010; accepted 13 Apr 2010; published 2 Jun 2010

Table 1. Effects of changing different dimensions on waveguide performance

Dimension	Effects of increasing the chosen dimension		
	Effective mode index	Propagation distance	Mode size
Waveguide width (w)	Increases	Decreases	Decreases
High index slab height (h)	Increases	Decreases	Decreases
Spacer height (d)	Decreases	Increases	Increases

Table 2. presents the dimensions chosen for the final design and the material properties at 800 nm for the different materials. Propagation distance in this case is 43 μm and the mode size is 350 nm. We take this as a reasonable compromise between confinement and propagation distance. Analysis for the rest of the paper is carried out for these dimensions and material properties unless otherwise stated.

Table 2. Details of material properties and waveguide dimensions for the finite width hybrid waveguide

Wavelength	0.8 μm
Material properties	$\varepsilon_{metal} = -32.8 + i0.46$(silver), $\varepsilon_{spacer} = 2.11$(silica) $\varepsilon_{hi} = 13.77 + i0.063$ (silicon), $\varepsilon_{cover} = 1$ (air)
Waveguide dimensions	w = 100 nm, h = 60 nm, d = 100 nm

Figure 6 shows the guided power density for the chosen parameters. Power is highly concentrated in the spacer layer.

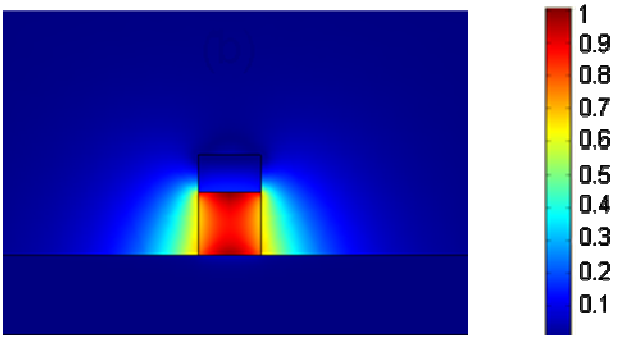

Fig. 6. Normalized guided power density of the hybrid mode for the parameters mentioned in Table 2.

The waveguide dispersion for the wavelength range of 0.5 to 1.2 μm is shown in Fig. 7. The dispersions of silica [20], silicon [20], and silver [17], [18] have been taken into account. As shown in Fig. 7(a), the mode is tightly confined at shorter wavelengths while confinement becomes worse for longer wavelengths. This is expected since for longer wavelength the guide becomes narrower in terms of wavelength of operation. Figure 7(b) presents the variations of real part of the mode effective index and propagation distance as a function of wavelength. For longer wavelengths the mode penetrates deeper into air and real part of effective mode index Re{n_{eff}} approaches 1. Like other plasmonic guides, there is a trade off between the propagation distance and confinement for the hybrid waveguide. As shown in Fig. 7(b), loss of confinement is accompanied by an increase of propagation distance.

#125806 - $15.00 USD Received 22 Mar 2010; revised 13 Apr 2010; accepted 13 Apr 2010; published 2 Jun 2010

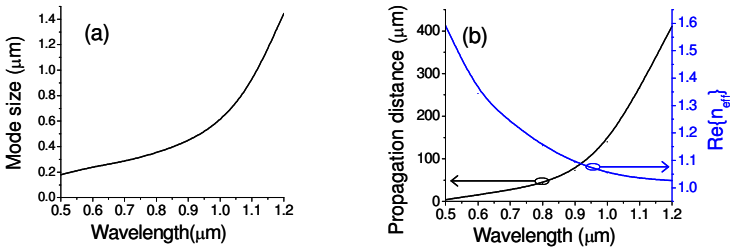

Fig. 7. Dispersion of the proposed guide for waveguide dimensions mentioned in Table 2. (a) mode size (b) propagation distance and real part of effective mode index.

Fabrication of the structure described above will require deposition of silica on a metal surface followed by deposition of silicon on top of silica and subsequent etching of these two layers. An alternate and easier fabrication process would be to implement the hybrid waveguide on SOI wafer as shown in Fig. 8(a). The fabrication steps will be selective etching of top silicon layer of the SOI wafer to define the high index region followed by deposition of silica and metal. Cover medium i.e. the medium around the hybrid guide in this case will be silica instead of air. Hybrid mode guided by such a guide is shown in Fig. 8(b).

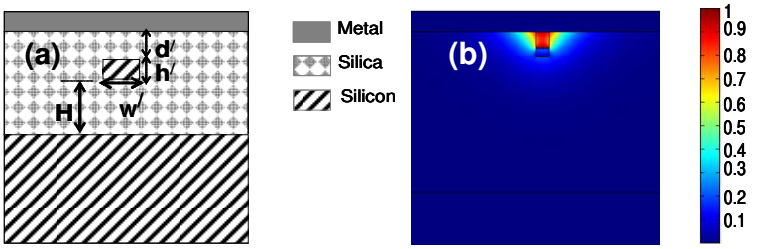

Fig. 8. (a) Schematic of the two dimensional hybrid guide on SOI wafer (b) normalized guided power density for waveguide dimensions $w' = 100$ nm, $h' = 60$ nm, $d' = 100$ nm, $H = 1$ μm.

We have investigated the effects of varying the permittivity of the cover region and show these results in Fig. 9. As shown in Fig. 9(a) an increase in ε_{cover} results in loss of confinement and increase of mode size. This loss of confinement is accompanied by an increase in the effective mode index n_{eff} as shown in Fig. 9(b). Propagation distance reaches a maximum when ε_{cover} is approximately equal to ε_{spacer}. At 800 nm wavelength silicon has a complex permittivity and the resulting loss is appreciable. To examine the effect of material loss of silicon on overall propagation distance we have also plotted the propagation distance in absence of silicon loss. While silicon loss plays an important role in limiting the propagation distance, metal loss is the main limiting factor.

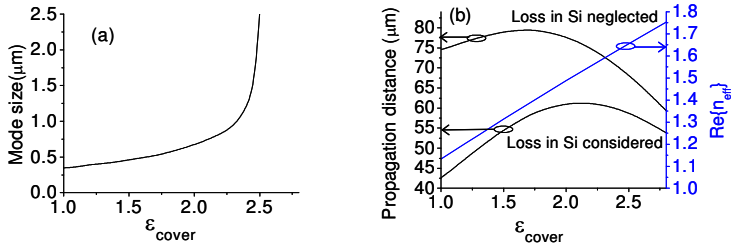

Fig. 9. Variations of the hybrid mode characteristics with the permittivity of surrounding medium for waveguide dimensions mentioned in Table 2. (a) mode size (b) propagation distance and real part of effective mode index.

#125806 - $15.00 USD Received 22 Mar 2010; revised 13 Apr 2010; accepted 13 Apr 2010; published 2 Jun 2010

The variation of propagation distance for the hybrid mode differs significantly from that of single interface SP mode. The propagation distance of the SP at a single metal-dielectric interface (δ_{sp}) is given by [21].

$$\delta_{SP} = \frac{1}{k_0}\left(\frac{\varepsilon_m' + \varepsilon_d}{\varepsilon_m' \varepsilon_d}\right)^{3/2} \frac{(\varepsilon_m')^2}{\varepsilon_m''} \tag{2}$$

Here ε_m' and ε_m'' are the real and imaginary parts of the metal permittivity and ε_d is the permittivity of the dielectric medium adjacent to the metal. The variation of δ_{SP} for a silver dielectric interface at 0.8 μm wavelength is shown Fig. 10. Unlike the case of hybrid mode, propagation distance in this case drops monotonically with increasing ε_d. For example when ε_d increases from 1 to 2, δ_{SP} drops by almost 65%. In contrast, Fig. 9(b) shows that for the hybrid waveguide structure propagation distance changes by less than 24% for same change in ε_{cover}. Also instead of changing monotonically, propagation distance becomes maximum for an optimum choice of ε_{cover}.

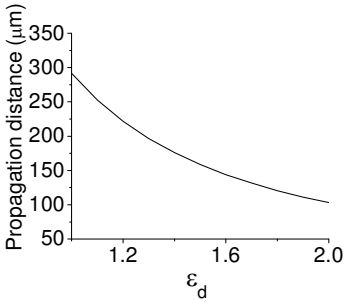

Fig. 10. Variation of propagation distance for SP at silver-dielectric interface as a function of permittivity of the dielectric medium

From the discussions of this section we can identify the following attractive features of the hybrid mode: (1) it can guide power in more confined fashion compared to single interface SP mode for the same propagation distance, (2) power is highly concentrated in low index spacer layer and (3) the propagation distance of the mode is relatively insensitive to change in permittivity of the cover layer.

3. Waveguide bends

Optical bends are often encountered in practical photonic circuits and their proper design is essential to the efficient operation of the circuit. To investigate the ability of the hybrid waveguide bend to guide light, in the following we will carry out a detailed study of such a structure using a commercial FDTD code by Lumerical [22]. All the waveguide dimensions are same as those mentioned in Table. 2. The size of the computational volume is 10μm × 10μm × 2μm and is truncated by perfectly matched layer boundaries. A uniform grid of 10 nm through out the computational volume is used.

Figure 11(a) shows transmission as a function of bend radius using air as the cover material. Here transmission is defined as the ratio of power at the end and beginning of the bend. Significant power transmission occurs even for sub-micron bend radius. Previous works on silica ridge on gold substrate reported complete loss of transmission for such bends [9]. It was also reported that ridge width less than 300 nm fails to confine the SP mode. In case of hybrid waveguide we achieve more than 46% transmission through a 90 degree bend having bend radius of 1 μm and waveguide width of 100 nm. The results reported here, therefore, indicate a significant improvement in performance. This is not unexpected. Since the proposed structure uses silicon in addition to silica, the guiding capability is expected to be enhanced. The guiding ability of hybrid waveguide bend is not very strong compared to that

#125806 - $15.00 USD Received 22 Mar 2010; revised 13 Apr 2010; accepted 13 Apr 2010; published 2 Jun 2010

of SOI nanowire bends. However, the application areas of the plasmonic waveguides and SOI nanowires most likely will be different. Surface plasmon offers a very high field intensity and the presence of metal makes surface functionalization by biological molecules relatively easy. These are some of the reasons for the popularity of plasmonics for bio-sensing. Since potential applications of plasmonic guides and SOI nanowires are different, we think it is reasonable to compare the performance of our proposed device with similar plasmonic guides instead of SOI nanowires.

In Section 2.2 we mentioned that propagation distance is larger and fabrication process is simpler when the cover region is silica instead of air. However, this increased propagation distance and reduced fabrication complexity come at the cost of diminished mode confinement. Such reduction in confinement may significantly increase the leakage loss especially in case of bends with small bend radii. To investigate the effect of cover layer on bend losses, we show the transmission as a function of bend radii when cover material is silica in Fig. 11(b). All other parameters are same as those of Fig. 11(a). From the figure it is clear that transmission is much worse when the cover material is silica.

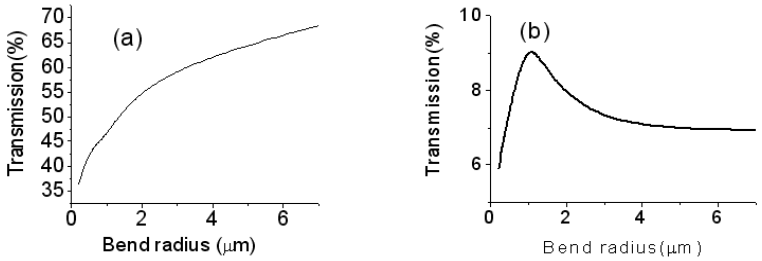

Fig. 11. Transmission through 90 degree bends for different bend radii for two different cover materials (a) air (b) silica. Spacer medium is silica for both straight and bend sections.

The difference between the transmissions in the two cases is illustrated further in Fig. 12(a) and 12(b). Here, we have plotted the *y*-component of the electric field (E_y) for a 1.5 μm bend with air [Fig. 12(a)] and silica [Fig. 12(b)] cover layers. This field quantity is chosen since it is responsible for the power flow and has similar field profile as the guided power. As Fig. 12(b) indicates, barely any power is transmitted when silica is the cover material.

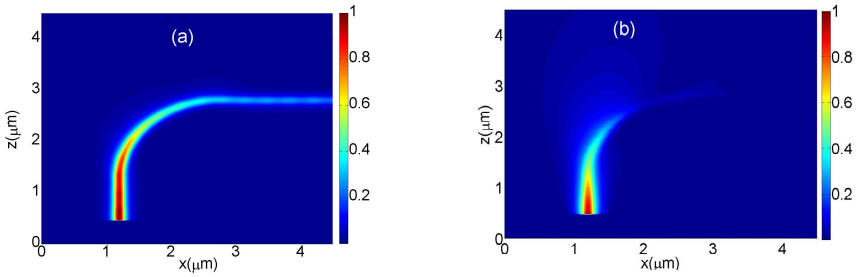

Fig. 12. E_y field intensity for a 90 degree bend with bend radius 1.5 μm when cover medium is (a) air (b) silica. Spacer layer is silica for both straight and bend sections.

One possible way to do reduce bend loss is to use a spacer layer of higher permittivity to increase confinement and reduce leakage radiation, but this would also increase material loss and hence reduces the propagation distance. For example, if the spacer layer for the straight waveguide described in Table. 2 is changed from silica to silicon nitride; propagation distance will reduce from 43 μm to 21 μm. A more promising solution would be to use a spacer layer of higher permittivity only in the bend section to reduce bend loss and to use a spacer with lower permittivity in the straight waveguide sections to minimize overall propagation loss. Figure 13 shows the transmission for different bend radii for this scheme. The waveguide

#125806 - $15.00 USD Received 22 Mar 2010; revised 13 Apr 2010; accepted 13 Apr 2010; published 2 Jun 2010

structure is same as that of Fig. 11 but with silicon nitride (ε_{spacer} = 4) spacer layer in the bend region and silica spacer layer in the straight waveguide section. Transmission is significantly enhanced for both cover material i.e. air and silica.

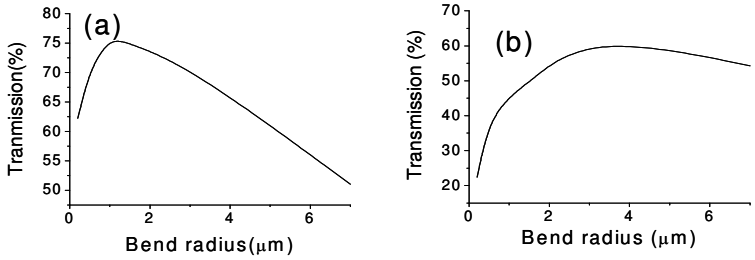

Fig. 13. Transmission through 90 degree bend for different bend radii for two different cover materials (a) air (b) silica. Spacer is silicon nitride in bend and silica in straight sections.

The effect of the silicon nitride spacer is further illustrated in Fig. 14. The structure is same as that shown in Fig. 12 but the spacer layer is now silicon nitride in the bend region. A standing wave is formed in the bend region because of index mismatch between bend and straight section but an improvement in transmission is evident.

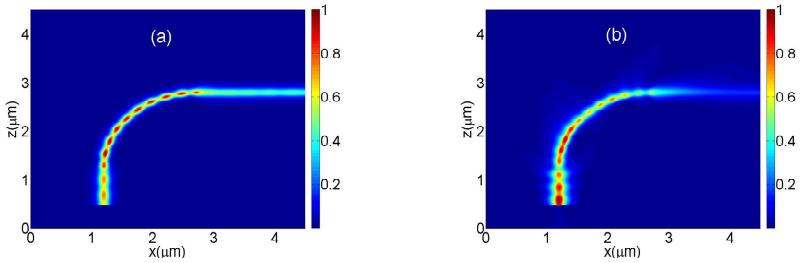

Fig. 14. E_y field intensity for a 90 degree bend with bend radius of 1.5 μm when cover medium is (a) air (b) silica. Spacer layer is silica nitride in bend and silica is straight sections.

For plasmonic waveguide bend, there is a trade off between propagation loss and radiation loss. Increase in mode confinement will result in reduced radiation loss. However, as the results of the parametric study in section 2 shows, increase in mode confinement also results in increased propagation loss. Transmission through bend reaches a maximum for an optimum bend radius. Waveguide dimensions, material properties and bend radius should be properly chosen to simultaneously achieve good confinement and high transmission through bends.

4. Conclusions

The properties of the hybrid mode guided by the waveguide consisting of a high dielectric medium adjacent to a metal plane with a thin low dielectric spacer are investigated. Power is concentrated in the low index spacer region for this waveguide. The hybrid waveguide is capable of guiding light efficiently through sub-micron bends. A design including the use of two different spacer materials in straight and bend sections is proposed to minimize bend loss. In addition to the capability of guiding light through tight bends, the hybrid guiding scheme offers a number of additional advantages. By suitable choice of materials it can be made compatible with silicon on insulator technology. It has high field intensity in the low index spacer layer and hence can be useful for sensing applications. More work is necessary to fully evaluate the potential of the hybrid wave guiding scheme for practical applications.

#125806 - $15.00 USD Received 22 Mar 2010; revised 13 Apr 2010; accepted 13 Apr 2010; published 2 Jun 2010